

# The Physical Limnology and Sedimentology of Meziadin Lake, Northern British Columbia, Canada

Robert Gilbert

Richard D. Butler

Department of Geography,  
Queen's University, Kingston,  
ON K7L 3N6, Canada.  
gilbert@lake.geog.queensu.ca

## Abstract

Meziadin Lake (34 km<sup>2</sup>, 133 m maximum depth) is located on the east side of the Coast Mountains in northern British Columbia. Inflow from Strohn Creek is dominated by the nival flood, despite a glacier cover of 50.5 km<sup>2</sup> in the drainage basin. The nival flood generates turbid underflows in the lake that distribute sandy mud within 2 km of the point of inflow. During our study in 1999, turbidity currents and interflows along the thermocline continued intermittently through the summer, although the inflow of water and the suspended sediment loads decreased substantially. Sediment collected in traps throughout the lake indicate mass accumulation rates in the proximal region in excess of 200 g m<sup>-2</sup> d<sup>-1</sup> (11 mm) averaged over 69 d of observation during summer 1999, decreasing downlake to 1 g m<sup>-2</sup> d<sup>-1</sup> (0.06 mm) in the most distal region of the lake. The sediment trapped near the point of inflow has a strong mode of fine sand and is strongly negatively skewed, reflecting the competence of the turbidity currents. Texture of the sediments deposited on the lake floor decreases distally from material dominated by coarse silt and fine sand to clay sized material. Sub-bottom acoustic data document more than 180 m of accumulation in the proximal region, decreasing to <20 m distally, making the mean rates of accumulation since deglaciation (16 and 1.8 mm yr<sup>-1</sup>, respectively) somewhat greater than those at present. This decrease is associated with changing environmental conditions and diversion of a significant portion of the drainage basin associated with the retreat of Strohn Glacier in the 20th century.

## Introduction

The fiord lakes of the Canadian Cordillera contain seasonally distinct sedimentary records, modified by the processes and landforms within their drainage basins (Gilbert et al., 1997) and conditioned by unique limnologic characteristics (Smith, 1978; Sturm, 1979). Lacustrine sedimentary records of montane lakes contain proxy evidence of environmental variability, including glacial history, and geomorphic and fluvial processes, all controlled by changing climate. Changes to climatic (Leemann and Niessen, 1994), hydrologic (Desloges and Gilbert, 1994), and glacial regimes (Leonard, 1986) have continued influence on those systems associated with interaction of lake and river water masses. These include water column structure and stability (Gilbert, 1975; Carmack et al., 1979), inflow-induced circulation (Hamblin and Carmack, 1978), and the relative importance of interflowing and underflowing density currents as depositional agents (Sturm and Matter, 1978). This paper assesses processes that affect the hydrology, limnology, and sedimentology of Meziadin Lake and its basin to provide a basis for comparison to large alpine systems elsewhere.

## Study Site

The regional climate of northwestern coastal British Columbia results from the interaction of Pacific and continental air masses (Cayan et al., 1989), the former driven by short-term oceanic and atmospheric oscillations (Ware and Thompson, 2000). These synoptic weather patterns are further modified by the complex physiography of the Cordillera (Ryder, 1989). Surface runoff is strongly seasonal, controlled primarily by nival and glacial melt, thereby providing temporal variation in the transportation and deposition of sediment. Precipitation especially

is spatially variable as a function of orographic processes in the Coast Ranges and is dominated by high winter snowfall (Gilbert et al., 1997).

Meziadin Lake is a deep glacial lake in the Nass Basin at the eastern edge of the Boundary Ranges in the northern Coast Mountains, a region characterized by significant area of present-day glaciers (Fig. 1). Strohn Creek and its tributary, Surprise Creek, are the most significant sources of sediment input to the lake because of the high relief of their basins and the glaciers in their headwaters (Fig. 1). Glaciers presently extend well below treeline, but since the Little Ice Age they have retreated significantly in the 20th century (Barnes, 2003), exposing moraines that continue to be sources of paraglacial sediment (Church and Ryder, 1972). Hannah and Tintina creeks are smaller meandering streams that drain the northeastern and eastern portions of the catchment in the Nass Basin, an area of low relief dominated by densely vegetated fens and bogs.

Meziadin Lake is 18.5 km long and a near uniform 2 km wide. Strohn Creek delta slopes steeply at 18° to 50-m depth (Fig. 2). The inflow-proximal basin is U-shaped with a flat, sediment-filled lake floor between 0.8 and 11 km from point of inflow. Maximum depth reaches 133 m. In the distal region, the lake is shallower and the bathymetry is more irregular as the thinner sediment fill incompletely masks the irregular bedrock topography beneath, as discussed below.

## Methods

In preparation for this study a sub-bottom acoustic survey was carried out in Meziadin Lake in 1998 using a Datasonics (Benthos) 3.5-kHz analogue system (Gilbert et al., 1997). Transects totaling 60.3 km were controlled by a single global position receiver and are accurate to ±30 m. The results were used to prepare a bathymetric map of the lake

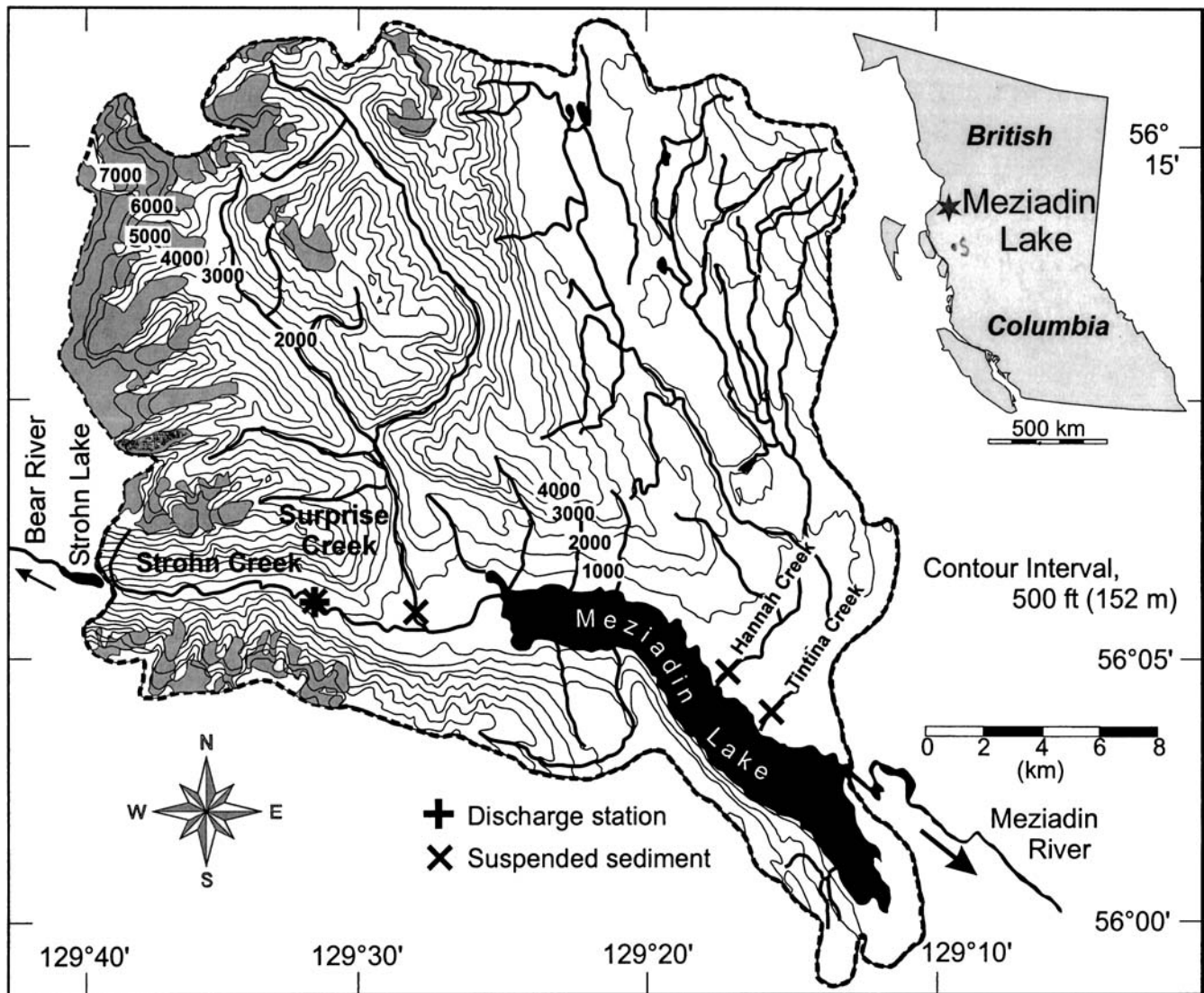


FIGURE 1. Meziadin Lake (34 km<sup>2</sup>, 244 m above sea level) and its drainage basin (530 km<sup>2</sup>). The largest inflow of water comes from the Strohn Creek drainage, including its tributary Surprise Creek (230 km<sup>2</sup>, of which 50.5 km<sup>2</sup> [22%] is glacier covered [gray shading on map]). Inset map of British Columbia indicates the location of the lake.

(Fig. 2) and assess the nature of the sediment fill in the lake, as described below.

The main period of fieldwork between 20 May and 10 August 1999 involved assessing the inflow of water and sediment to the lake, measuring lacustrine processes, and recovering short cores of sediment from the lake floor (Figs. 1 and 2). Air temperature and precipitation were logged at lake level. Mean daily air temperatures were best correlated with records from Smithers ( $r^2 = 0.93$ ), located 200 km south of Meziadin Lake. These were used to extend the short-term Meziadin Lake data. Strohn Creek upstream of Surprise Creek was measured by standard current metering techniques (Corbett, 1962) related to the stage records to produce a hydrograph of discharge. Measurements were made before, during, and after the nival flood to ensure the stability of the rating curve. Suspended sediment concentration was determined from depth-integrated samples recovered from Strohn, Surprise, Hanna, and Tintina creeks (Fig. 1) and filtered through 0.45- $\mu$ m cellulosic membrane on site.

Profiles of water temperature, conductivity, and optical turbidity were taken at 18 sites through the field season in Meziadin Lake (Fig. 2) using a Hydrolab Datasonde3. Suspended sediment concentration in the water column was determined from optical transmissivity using the

relation established in nearby Bowser Lake (Gilbert et al., 1997). To assess the frequency of turbid underflows that are warmer than the hypolimnion (cf. Gilbert, 1975; Lewis et al., 2002), water temperature was continuously logged 1.5 m above the bottom from 12 June to 7 August at a site near the point of inflow (Fig. 2). Eleven sediment-trap moorings (Fig. 2) documented the flux of suspended sediment in Meziadin Lake between 4 or 6 June and 8 August. Each mooring consisted of paired funnel-shaped traps set 1 m apart at 40-m depth and 1 m above the lake floor. Each of the 20-cm-diameter traps (cf. Lewis et al., 2002) was baffled at the mouth to increase trap efficiency (Gardner, 1980; Bale, 1998). Sediment accumulated in 0.5- or 1.0-L Nalgene bottles below each trap.

An Ekman grab was used to sample the lacustrine sediment in Meziadin Lake (Fig. 2). Undisturbed cores taken from the Ekman immediately after recovery were split, logged and photographed in the laboratory before being subsampled for determination of organic and inorganic content by loss on ignition (Dean, 1974) and grain size using a Coulter LS 200, laser scattering particle size analyzer. Similar procedures were used on the sediments obtained in the traps. Thin sections from the Ekman cores were prepared following Lamoureux (1994).

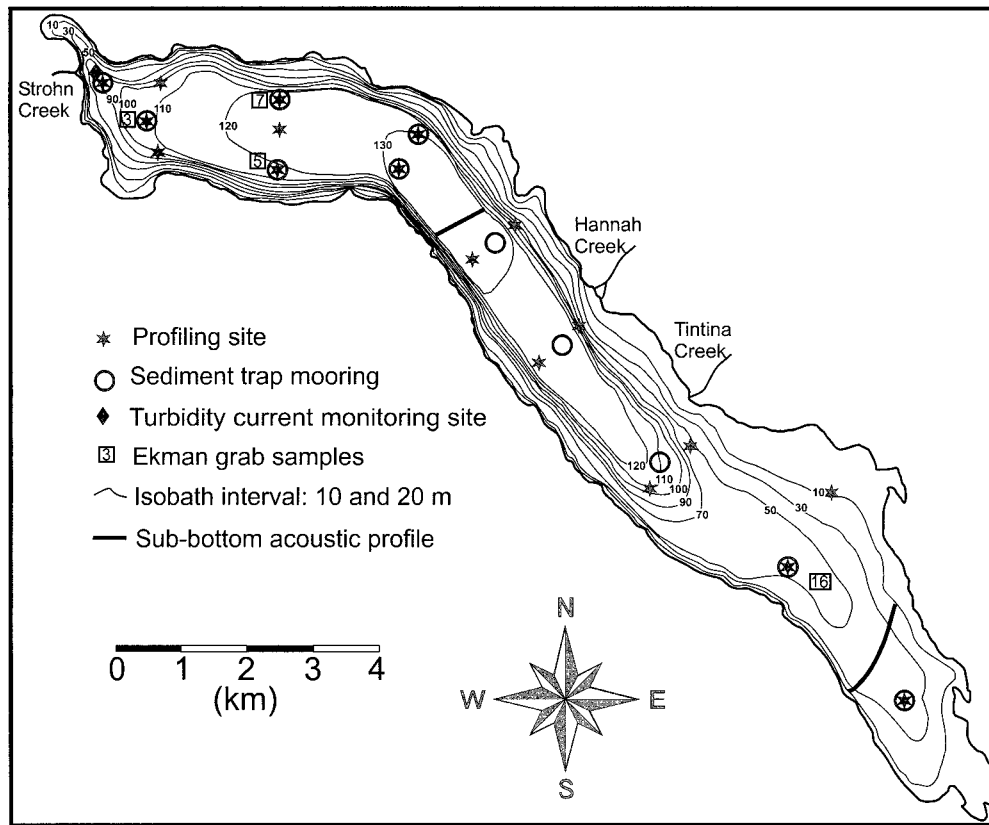


FIGURE 2. Bathymetry of Meziadin Lake based on 60.3 km of acoustic sub-bottom survey. Locations of profiles of water temperature, conductivity and optical turbidity, sediment-trap moorings, water temperature monitoring site, and Ekman grab samples are indicated.

Details of these methods and of the observations derived from them are provided by Butler (2001).

## Results and Interpretation

### INFLOW

The hydrograph of Strohn Creek discharge upstream of Surprise Creek (Fig. 3) shows a large nival peak driven by a period of warm air temperature and augmented by precipitation. Maximum discharge reached  $18.3 \text{ m}^3 \text{ s}^{-1}$  on 16 June, with mean flow through the study period of  $9.3 \text{ m}^3 \text{ s}^{-1}$ . Estimation of the discharge of Surprise Creek was made based on the Strohn Creek data scaled by the relative areas of the two basins. This linear extrapolation is justified on the basis of the similar morphology of the drainage basins, although it may overestimate discharge in the larger basin (Eaton et al., 2002). The results indicate that peak and mean flows entering Meziadin Lake during this period were approximately 80 and  $40 \text{ m}^3 \text{ s}^{-1}$ , respectively. The most important influence on discharge in the Meziadin basin, demonstrated by an  $r^2$  value of 0.45, was air temperature at Smithers, 200 km south. Leemann and Niessen (1994) also documented a positive correlation between air temperature (April to October) and runoff, with a correlation coefficient of 0.70 ( $r^2 = 0.49$ ) (see also Young, 1980; Röthlisberger and Lang, 1987). Diurnal variation in discharge caused by daily temperature fluctuation was not pronounced in early June but was significant in the later part of the summer, when discharge variation was almost completely a function of glacial melt with little or no nival component.

Suspended sediment concentrations (SSCs) in Surprise Creek were consistently greater than in Strohn Creek (Fig. 3), especially during the nival melt, when peaks of 1.425 and  $0.184 \text{ g L}^{-1}$  occurred, respectively. SSCs linked to discharge in each stream by means of rating curves and

multiplied by discharge produced an order-of-magnitude estimate of the total load of  $73 \times 10^3$  tonnes of suspended sediment delivered to Meziadin Lake during the 69-d study period. This is an amount sufficient to accumulate about 1.5 mm on the  $34 \text{ km}^2$  of lake floor. Since this represents much of the period of inflow, it is probable that mean annual accumulation was less than 2 mm, assuming a trap efficiency >95% (Brune, 1953). SSCs and especially discharge of Hanna and Tintina creeks were smaller than in Strohn Creek, and their combined input is an order of magnitude lower than in Strohn Creek.

### PHYSICAL LIMNOLOGY

While the entire lake within 3 km of the Strohn Creek inflow was isothermal near  $4^\circ\text{C}$  in early June, surface water in the more distal regions had already warmed to  $8^\circ\text{C}$ . Through the summer, surface water everywhere in the lake warmed to 14 to  $17^\circ\text{C}$  by August, with temperatures decreasing uniformly to 5 to  $6^\circ\text{C}$  between 40-m depth and the lake bottom. A distinct, well-mixed epilimnion did not develop anywhere despite the occurrence of katabatic winds reaching  $30\text{--}40 \text{ km h}^{-1}$  regularly during warm afternoons. During peak inflow in mid-June, water temperature below 40 m at sites within 6 km of the inflow was intermittently 1 to  $2^\circ\text{C}$  warmer than overlying water due to the underflow of warmer turbid river water (cf. Gilbert, 1975), as described below.

The patterns of SSC (Fig. 4) document the distribution of turbid water from Strohn Creek through the lake. With the onset of nival melt in early June (Fig. 3) and the development of thermal stratification in the distal parts of the lake, the presence of the first weak turbidity currents driven by SSCs of 20 to  $40 \text{ mg L}^{-1}$  could be detected (Fig. 4a). The nearly isothermal conditions in the proximal region of the lake led to mixing of these turbid waters through the water column as the current weakened. However, distally at 20- to 40-m depth in the lower

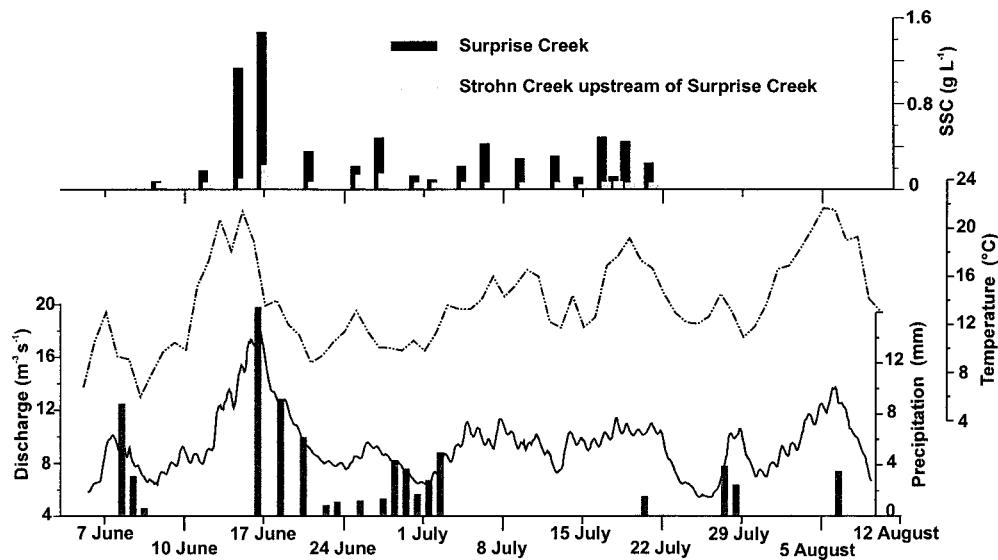


FIGURE 3. Discharge hydrograph for Strohn Creek and suspended sediment concentrations (SSCs) in Strohn and Surprise creeks at locations shown in Figure 1. Also shown is the mean daily air temperature at Smithers, 200 km south of Meziadin Lake.

region of the warming lake water, an interflow plume carried slightly more turbid water the length of the lake (Fig. 4a).

With the arrival of the nival flood and its significantly greater SSCs on 17 June, a strong turbidity current with sediment concentrations exceeding  $75 \text{ mg L}^{-1}$  occurred (Fig. 4b). Application of Middleton's (1966) formula with a coefficient of 0.4 expressing the ratio of interfacial to basal shear (van Tassel, 1981) suggests that the turbidity current had a mean velocity in the body of  $5\text{--}10 \text{ cm s}^{-1}$ . This is sufficient to transport sand but is not sufficient to erode sediments already deposited on the floor of the lake. This velocity is somewhat lower than those reported by Gustavson (1975), Lambert and Hsü (1979), Gilbert and Shaw (1981), Weirich (1986), and Lewis et al. (2002) in other glacial lakes. A cross-section at 5 km from the inflow on 17 June (Fig.

4b) showed that the slow-moving turbidity current was strongly directed to the south (right-hand) side of the basin under the influence of the Coriolis effect (cf. Carmack et al., 1979). SSCs in the turbidity current reached  $75 \text{ mg L}^{-1}$  while water along the north side at the same depth (120 m) contained 20 to  $30 \text{ mg L}^{-1}$ . Water near the surface in the midsection of the lake and throughout the distal portion of the lake actually became less turbid than a week earlier. It is possible that return flow along the surface drawn by interfacial shear along the plunging turbidity currents at this time (cf. Lambert et al., 1976; Pharo and Carmack, 1979) drew clearer water uplake, although no debris line was observed at the plunge point, as is the case where the process is well developed (Gilbert, 1975).

As the summer progressed, despite glacial melt, the discharge and SSCs were never as high as during the nival flood, although interflows and weak underflows both continued to occur, delivering water with SSCs from 30 to  $40 \text{ mg L}^{-1}$  throughout the lake (Fig. 4c). By August, both processes had weakened and the lake was clearing of its sediment load, especially distally, where SSCs decreased to  $<10 \text{ mg L}^{-1}$ . An important but poorly answered question in lacustrine sedimentology is how fine-grained sediment (mean in the clay size range—see below) is removed from the water column so quickly when Stokes Law indicates years to decades for settling. The roles of vertical circulation and flocculation (Droppo et al., 1997) are critical to these processes and to assessing the nature of the clay cap in varved glacialacustrine sediment.

An independent measure of the presence of turbidity currents in Meziadin Lake was provided by a nearly continuous record of temperature (Fig. 5) collected 1 m above the lake floor at a site near the point of inflow (Fig. 2) using a small, submersible data logger. While this does not provide velocity data, it does document inflow-generated turbidity current events when the river water is warmer than the ambient water at the bottom of the lake (Gilbert, 1975; Lambert and Giovanoli, 1988; Lewis et al., 2002). The nival flood was generating daily turbidity currents at least as early as 10 June. At this time, the suspended load was less than a few days later at the peak; in addition, the lake water was less turbid and thermal structure had not developed. Thus, flow was able to pass unimpeded along the lake floor. The wave pattern in the hypolimnion portion of the SSC profile of 17 June (Fig. 4) suggests subsequent passage of several turbidity currents. Following the peak inflow on 17 June, several daily pulses are evident (Fig. 5), and throughout much of the rest of June and July events lasting from less than one hour to several hours occurred regularly, each raising the water

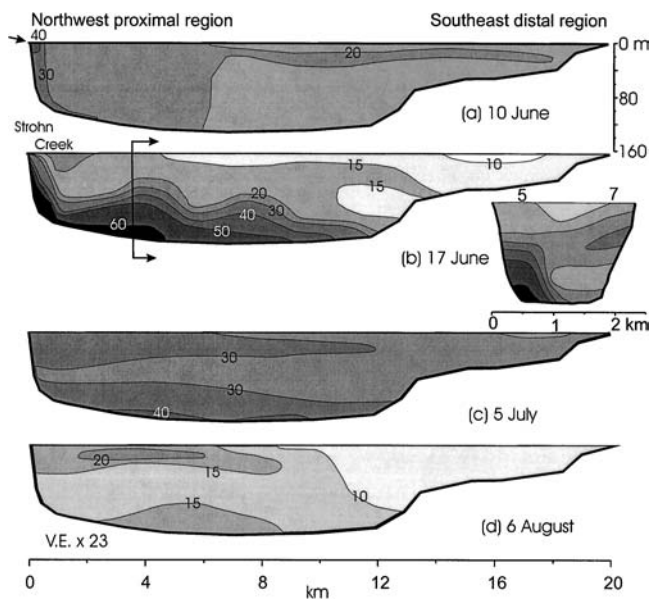


FIGURE 4. Transects along Meziadin Lake from the northwest (Strohn Creek inflow) to the southeast corner of the lake showing the suspended sediment concentration in  $\text{mg L}^{-1}$  determined from optical transmissivity and the calibration obtained in nearby Bowser Lake (Gilbert et al., 1997). Inset on 17 June shows the cross-lake data at stations 5 and 7 (Fig. 2).

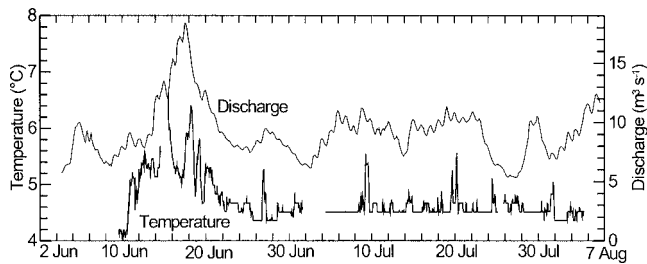


FIGURE 5. Discharge hydrograph for Strohn Creek and temperature 1 m above the lake floor at a site near the point of inflow (Fig. 2) illustrating the frequency of turbidity currents as peaks in temperature.

temperature measurably. Although turbidity currents in Meziadin Lake were not as regular as in lakes receiving a large input of suspended sediment (e.g., Gilbert 1975, 2000; Weirich, 1986), the temperature data indicate that underflow is an effective means of delivering water and sediment throughout the deepest regions of the lake.

#### LACUSTRINE SEDIMENTATION—TRAP RESULTS

Sediment traps were deployed on 11 moorings in the lake (Figs. 2 and 6) on 4 or 6 June and were recovered on 8 August (64 or 66 d later), each consisting of paired traps at 40-m depth and at 1 m above the lake floor. Mooring 9 was lost, and the lower traps on mooring 6 were damaged, probably associated with the sport fishery in the lake. The mass accumulation rates (MAR) shown in Figure 6 document the input of sediment from Strohn Creek and the lacustrine distribution processes described above. The mean bulk density of surficial sediments obtained in ten Ekman grabs ( $1210 \text{ kg m}^{-3}$ ) was used to convert MAR to the thickness of accumulation values shown in Figure 6.

MAR at 40-m depth was only 19 to 50% of that at the lake bottom, with the exception of the most proximal mooring (1), where it was 87%. This reflects both the greater water column above the lower traps from which sediment was settling and especially the higher SSCs in the lower water. The nearly equal accumulation in the traps at the proximal mooring only 300 m from the edge of the delta illustrates mixing of turbid water as the turbidity currents descended the foreset slopes of the delta (Fig. 4).

MAR decreases rapidly away from the delta, except that there appears to be some bypassing in the region about 4 km from the delta. Here the rates of accumulation both at 40 m and at the lake floor are less than in more distal traps and only about 5 to 10% of MAR in the proximal traps. It is in this region that, although the slope of the lake floor is small (Fig. 2), turbidity currents maintain much of their velocity due to inertia and are still able to transport most of their load. By moorings 5, 6, and 7 (Fig. 6), the floor is flat or rising and the currents are substantially slowed as they deposit more of their sediment here than at sites 3 and 4. Such distally increasing rates of accumulation have also been reported in other glacial lakes (Gilbert, 1975; Pickrill and Irwin, 1983; Gilbert and Desloges, 1987; Gilbert et al., 1997), although in Meziadin Lake this process appears to be occurring on a smaller scale. Beyond this region the decrease in MAR is consistent, with the most distal values in the range of a few grams per square meter per day.

Moorings 3 and 4 and moorings 5 and 6 were placed across the lake from each other so that the Coriolis effect could be examined. In each case, MAR on the south (right) side of the lake was significantly greater than on the north, varying from 2.39 and 2.12 times between moorings 3 and 4 at 40 m and 1 m from the bottom, respectively, and 1.54 times between moorings 5 and 6, 1 m from the bottom.

Because we anticipated that the most proximal traps would fill rapidly, moorings 1 and 2 were recovered on 3 July, about 2 wk after the nival flood. All the sediment reservoirs on mooring 1 and the lower reservoirs on mooring 2 were replaced, and the moorings were reset

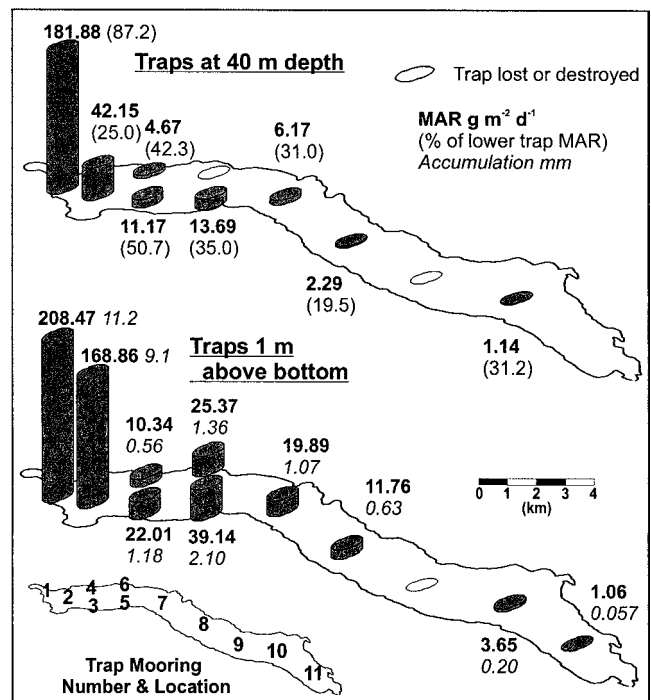


FIGURE 6. Mass accumulation rates (MARs) in Meziadin Lake from sediment traps located at 40-m depth and 1 m above the lake floor during the period 4 or 6 June to 8 August. Values of MAR (bold) represent the mean of 2 traps at each location. MAR in the upper traps is shown as a percentage of that in the lower traps at each site (parentheses). Accumulation during that period on the lake floor (italics) is derived from MAR based on a mean measured bulk density of  $1210 \text{ kg m}^{-3}$  in 10 surficial samples of the lake floor. Trap numbers refer to discussion in text. Only the lower traps were deployed at site 11 due to the shallow water depth.

immediately. In the 29-d period before 3 July, MAR at mooring 1 was  $324.3 \text{ g m}^{-2} \text{ d}^{-1}$  at 40-m depth and  $400.1 \text{ g m}^{-2} \text{ d}^{-1}$  1 m above the bottom; MAR at mooring 2 was  $346.2 \text{ g m}^{-2} \text{ d}^{-1}$  1 m above the bottom. This indicates the importance of the nival flood because these values are 92, 86, and 93%, respectively, of the total MAR during the 69-d study period. Pharo and Carmack (1979) reported that 90% of sediment input to Kamloops Lake occurred during the spring freshet. The rates of sediment accumulation on the lake floor calculated from MAR in traps 1 m from the lake floor vary from about 10 mm in the proximal area to as little as 0.06 mm in the most distal region. Clearly, we missed a small amount of accumulation in June before the nival melt and a greater amount into the autumn, but since our 64- to 66-d observation period covered most of the greatest inflow of water and sediment, the accumulation rates shown in Figure 6 probably represent most of the annual accumulation in the lake. Our estimate of accumulation from measurements of water and sediment in Strohn and Surprise creeks (Fig. 3) was that the sediment load during the measurement period should represent deposition of 1.5 mm averaged over the entire lake floor; this is in reasonable agreement with the sediment-trap results (Fig. 6).

Sufficient sediment accumulated in the proximal traps that the deposits could be treated as short cores (cf. Gilbert et al., 2003). The sediment appears massive in visual inspection of a cleaned surface, in thin section, and in x-radiographs, although there is no evidence of bioturbation as the sediment was deposited in the traps. However, the texture, as represented in the particle size distributions shown in Figure 7, is distinctive. The coarsest sediments were deposited in the traps at site 1 (Fig. 6) located 1 m above the lake floor and are associated with the most vigorous turbidity currents generated during the nival melt (Fig. 5). The strong mode centered on  $100 \mu\text{m}$  is most prominent at

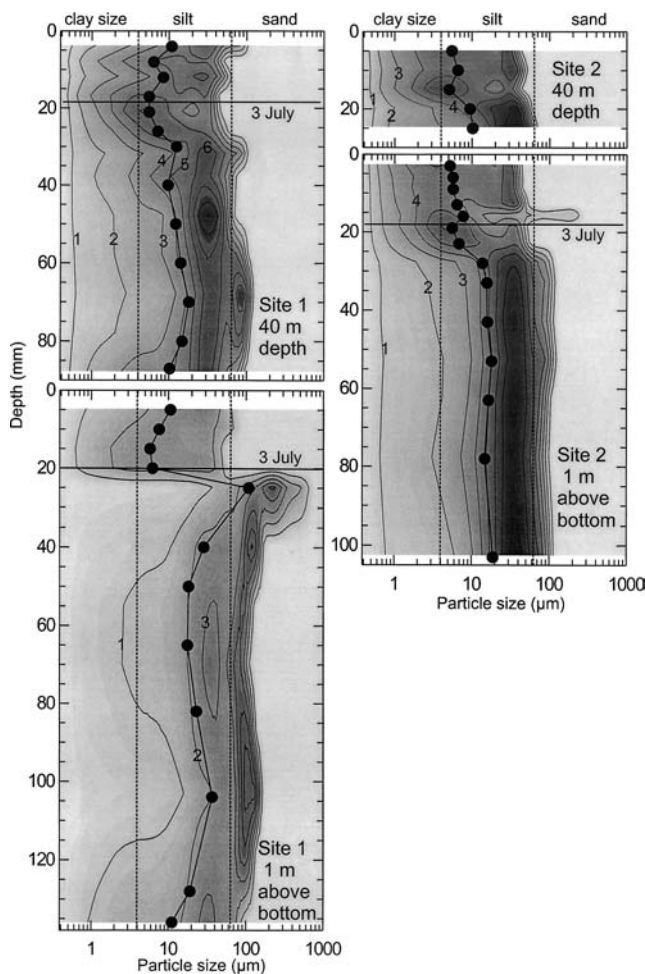


FIGURE 7. Particle size distributions (after Beierle et al., 2002) in sediment traps at sites 1 and 2 (Fig. 6). Values are in percent in 0.25 phi intervals; isopleth interval is 1%. Also shown is the geometric mean grain size (dots). Deposition began on 4 June and ended on 8 August when the traps were recovered. Reservoirs on 3 trap pairs were replaced on 3 July, providing a time marker as shown.

80- to 120-mm depth in the trapped sediment and may correspond to the largest turbidity currents on 18 to 21 June (Fig. 5). The particle size distributions are strongly negatively skewed ( $-0.8$  to  $-1.4$ ), reflecting the competence of the turbidity currents to transport fine sand but not particles of larger diameter (see estimated velocity values reported above). The sediment deposited shortly before recovery on 3 July may be an artifact of the recovery or handling process, since it does not correspond to observed processes in the lake, although there was no apparent disturbance or contamination of the sediment in the trap during or after recovery. After 3 July the sediment distribution is significantly finer (mean 5 to 12  $\mu\text{m}$ ) and the distribution is more symmetrical (skewness  $-0.1$  to  $-0.4$ ). Sand content decreases to a few percent as the effect of turbidity currents in this period diminishes (Fig. 5).

The sediment in the 40-m-deep trap at site 1 does not contain a mode in the fine sand range except for a brief period at 70 mm depth that probably also corresponds to the occurrence of the most vigorous turbidity currents. Even the secondary mode in midsilt size fades before early July, and the mean decreases from 18  $\mu\text{m}$  in mid-June to 5 to 11  $\mu\text{m}$  in July as in the lower traps, reflecting the shift from deposition predominantly from turbidity currents to deposition mostly of fine particles settling from suspension in interflows (Fig. 4).

At site 2, 1 km from the inflow, the sediment in the traps 1 m from the lake floor is finer and the mode has shifted from fine sand to coarse

silt size during the nival turbidity current events. The finer mean grain size (8 to 18  $\mu\text{m}$ ) and the only slight to moderate negative skewness of the particle size distribution ( $-1.0$  to  $-0.4$ ) indicate that a much larger component of the sediment deposited at this site is from suspension. The sediment deposited in July at the 1-m site and throughout the entire study period at 40-m depth became progressively finer through time (mean decreasing from 10 to 4  $\mu\text{m}$ ), and negative skewness decreased from  $-0.6$  to  $-0.1$ , suggesting increasing dominance of deposition from suspension. In traps at sites 1 and 2 the organic content determined by loss-on-ignition was 1 to 3%, illustrating the overwhelming role of clastic sedimentation in the proximal region.

These data in combination with the MAR (Fig. 6) indicate that the effectiveness of turbidity currents decreases rapidly within the first kilometer in the lake, where the rates of deposition are up to 20 times higher than more distally, but that weak currents are sufficient to allow some bypassing in the region centered 2 km from the inflow before greater deposition occurs about 4 km downlake, associated with the final weakening of underflow. Distally from there, rates continue to decrease to the end of the lake.

#### LACUSTRINE SEDIMENTATION—SHORT CORES

Four of the short cores of surficial sediment obtained from Ekman grab samples confirm the sedimentary processes documented above. Ekman 3 represents sediments within 1 km of the inflow of Strohn Creek (Fig. 1). Rhythmic couplets averaging 12 to 17 mm thick consist of a silt- and clay-rich lamina 1 to 2 mm thick and a coarser-grained deposit consisting of a series of laminae poorly distinguished by color and texture. These are not the classic varves of most glacial lakes, although the approximate correspondence with the rate of accumulation in the sediment traps in this region (Fig. 6) suggests that these are indeed annual deposits. Mean grain size (Fig. 8) is in the silt range, corresponding to the sediment in traps at site 2, which is nearest this location (Figs. 6 and 7). Both the trap and lake floor sediment in this region are negatively skewed ( $-0.4$  to  $-1.2$ ) with 5 to 20% fine sand, although in lake floor samples containing sediment from the fine (probably winter) laminae, the skewness becomes neutral or slightly positive (0 to 0.3) as a consequence of the deposition of this fine sediment by slow settling from suspension.

Ekman 5 and 7 represent the sedimentary environment about 3 km from the inflow. Here laminae are still visible both in the exposed split surface of the core and in thin section, but the layers are of irregular thickness from  $>1$  to 5 mm thick, and no annual signal can be distinguished. The laminae are probably the result of irregular underflow events that reach this section of the lake. In this region they slow as they pass over the nearly horizontal lake floor and so deposit the finer-grained material as their competence decreases. These are difficult to distinguish from the fine-grained materials deposited from suspension, including during the winter. The mean grain size of the sediment in this region is in the fine silt and coarse clay size range (Fig. 8). The result of deflection of flow to the south (right) of the lake by the Coriolis effect is apparent in the grain size results. Sediments in Ekman 5 (right side) have slightly coarser grain size than those of Ekman 7, a much higher proportion of silt, and less than 1% sand, whereas those at Ekman 7 have no sand.

The upper 100 mm of Ekman 5 contain significantly coarser sediment than in the material below (Fig. 8). The trap data indicate a rate of accumulation of about 1 to 2  $\text{mm yr}^{-1}$  in this region (Fig. 6), suggesting that this upper sediment may represent much of the 20th century. This is the period of post-Little Ice Age glacial retreat (Clague and Mathewes, 1996; Barnes, 2003), which is associated with more rapid rates of meltwater production and greater availability of sediment from retreating glaciers and the land surfaces newly exposed by retreat. This phenomenon of higher sediment production during retreat has

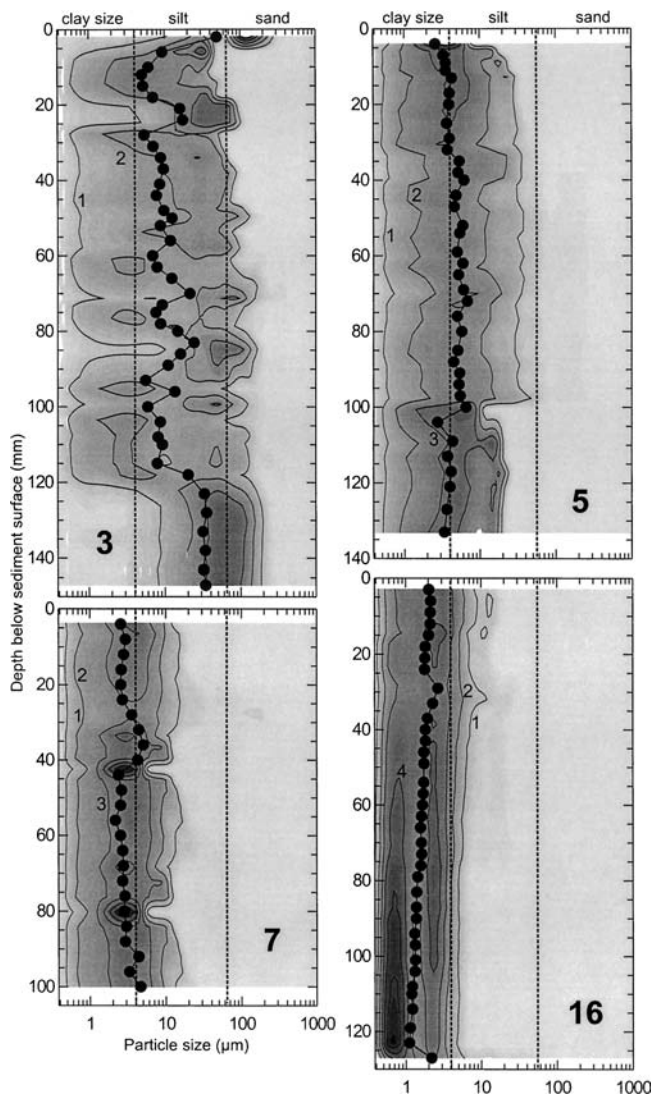


FIGURE 8. Particle size distributions (after Beierle et al., 2002) in four Ekman samples of surficial sediments from Meziadin Lake. Values are in percent in 0.25 phi intervals; isopleth interval is 1%. Also shown is the geometric mean grain size (dots). For locations see Figure 2.

been noted by Leonard (1997) and others and is important in assessing sediment budgets of glaciated terrain.

In the distal environment as represented by Ekman 16 (Fig. 2), the sediment is entirely massive and very fine grained, with the mean grain size in the range of mean clay size to fine silt (Fig. 8). Coarse silt and sand are absent. Trap data indicate rates of accumulation of a small fraction of a millimeter per year, suggesting that the 127 mm of Ekman 16 constitute at least several centuries of accumulation, including most or all of the Little Ice Age. Texture of sediment has increased steadily through this period from a mean at 120 mm of 1.2  $\mu\text{m}$  to 1.8 to 2.8  $\mu\text{m}$  above 40-mm depth. Below 60 mm there is a strong mode in the fine-clay size range (<1  $\mu\text{m}$ ); however, from about 110 m upward this is gradually replaced by a mode in the coarse clay size (2–4  $\mu\text{m}$ ). The finer mode disappears about 60-mm depth and a small fraction of fine to medium silt appears, forming a secondary mode in the upper 10 mm (Fig. 8). This also supports the contention of very little sediment input during the Little Ice Age but an increasingly dynamic environment with more coarse sediment (and probably greater amounts of sediment) since.

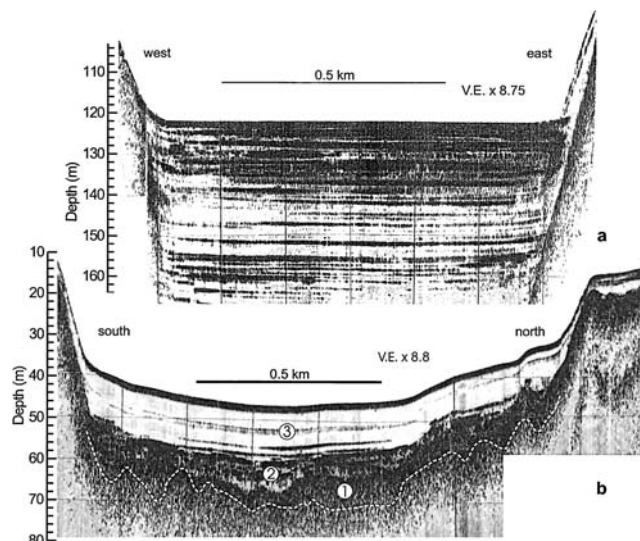


FIGURE 9. 3.5 kHz sub-bottom acoustic profiles (a) in the inflow-proximal region and (b) in the distal region of Meziadin Lake. Locations are shown on Figure 2. Depths in water and sediment assume a sound velocity of 1460  $\text{m s}^{-1}$ . Numbers refer to acoustic facies described in the text. The dashed line marks the lowest reflecting surface interpreted as bedrock.

#### LACUSTRINE SEDIMENTATION—ACOUSTIC DATA

The sub-bottom acoustic survey provides evidence of the sedimentary processes described above and of the sedimentary history of Meziadin Lake. Within 3 to 4 km of the Strohn Creek delta, sandy sediment prevented acoustic penetration, and the only data in this region are of bathymetry and lake floor morphology (cf. Gilbert and Desloges, 1992; Gilbert et al., 1997; Desloges and Gilbert, 1998; Lewis et al., 2002). The deepest part of the lake beyond this region consists of steep side walls having a thin cover of sediment (<10 m) and a flat lake floor of acoustically laminated sediment in which sound penetration was everywhere more than 50 m (Fig. 9a). This signal is characteristic of lakes and marine environments with moderate to high rates of deposition of underconsolidated fine-grained sediments (silt and clay size) that have high water contents. Episodic turbidity currents spread coarser-grained sediments (up to 30% fine sand) widely across the lake floor, creating more reflective surfaces that can be traced across the lake (despite the evidence of the Coriolis effect reported above) and in some cases for more than 10 km downlake (cf. Gilbert et al., 1997). These internal reflectors are largely absent from the side walls (Fig. 9a) because turbidity currents probably do not extend up the side walls in this portion of the lake.

In the deepest portion of the lake, the sediment was too thick to be completely penetrated to bedrock. However, the lowest strong reflector in the side wall interpreted as the bedrock surface was extended beneath the lake floor by fitting a parabola to each transect where this occurred (cf. Gilbert et al., 1997). From this we interpret that the maximum sediment thickness is about  $185 \pm 20$  m (Fig. 10). This is less than the sediment thickness of 234 m calculated in the same way for nearby Bowser Lake (Gilbert et al., 1997).

In the distal part of the lake (Fig. 9b), sediment accumulation is much less and penetration to bedrock occurred almost everywhere. Three acoustic facies can be recognized. Facies 1 is an irregular deposit that is almost impenetrable and difficult to distinguish from the lowest reflector interpreted as bedrock. Facies 2 is more acoustically transparent, with numerous strong internal reflectors; its thickness varies as it infills and smooths depressions in Facies 1. Facies 3 is an acoustically transparent deposit of more uniform thickness conformably

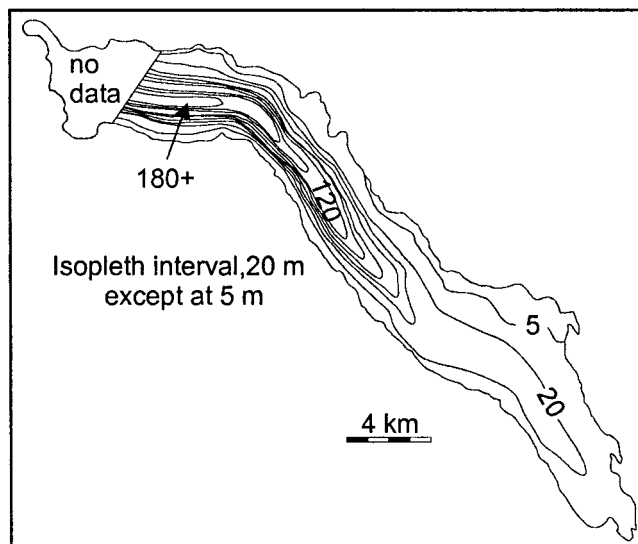


FIGURE 10. Total thickness of sediment in Meziadin Lake determined from sub-bottom acoustic survey.

overlying the sediment beneath. Only a few minor reflectors occur in Facies 3.

Facies 1 is interpreted as an ice-proximal or ice-contact sediment deposited during deglaciation, when the lake basin was still occupied by a glacier. Facies 2 represents the early phase of Meziadin Lake as the glacier was retreating but probably still occupied part of the lacustrine basin. The sharp transition between facies 2 and 3 may relate to the rapid retreat of Pleistocene glaciers in the Cordillera (Clague and Evans, 1993). Facies 3 represents the Holocene environment of Meziadin Lake similar to that of the present. Except for several weak reflectors, facies 3 is acoustically unstratified in the distal region of the lake because turbidity currents do not reach this area, being unable to travel up the reverse slope from the deepest part of the lake, and so the coarser sediments that provide reflectors are absent. The acoustic data from the proximal region (Fig. 9a) show a zone from about 22 to 36 m below the sediment surface in which there are fewer reflectors. This may represent a time of reduced turbidity current activity associated with mid-Holocene warmer conditions in the drainage basin. Thus, glaciers were probably smaller and contributed less water and sediment to Meziadin Lake.

The thickness of the lacustrine sediment in Meziadin Lake (Fig. 10) provides a measure of the mean rate of accumulation in the approximately 11 ka since deglaciation (Ryder and Maynard, 1991). A thickness of 185 m represents accumulation of about  $17 \text{ mm yr}^{-1}$  in the proximal region, which may be compared to the rates of 9 to  $11 \text{ mm yr}^{-1}$  collected in the sediment traps placed in 1999. In the distal region, accumulation of facies 3 (postglacial lacustrine sediment) is less than 12 m, representing an average of less than  $\sim 1 \text{ mm yr}^{-1}$  compared with the rate in 1999 of 0.06 to  $0.2 \text{ mm yr}^{-1}$ . The higher historical rate is associated with (1) sediment recovery in traps not representing a complete year, (2) the loss of contribution of sediment from Strohn Glacier via Strohn Lake, and (3) variability of sediment input due to climatically controlled glacier activity and the paraglacial effect (Ballantyne, 2002) as Pleistocene and early Holocene sediment supplies decreased following deglaciation. Strohn Glacier (area  $30.3 \text{ km}^2$ ) filled the headwater region of Strohn Creek until the 1930s and contributed water and sediment to both Strohn Creek and westward to the Bear River drainage and thence to Portland Canal at Stewart (Mathews, 1965). Subsequent retreat created ice-dammed Strohn Lake (Fig. 1) within the terminal moraine. Water continued to flow both east (80% of the discharge) and west, although the eastward flow to Strohn

Creek would have carried less sediment due to the trapping effect of the lake. The lake drained catastrophically into Bear River five times between 1958 and 1962 (Mathews, 1965); since then the dam has not re-formed, and all flow from the 43.1-km drainage area has been into the Bear River. The loss of this area (15% of the Strohn Creek drainage, 37% of the area glacier covered) represented a significant reduction in sediment supply.

## Conclusions

Meziadin Lake is one of a group of large fiord lakes in the Cordillera having modest inflow of water and sediment from glacial sources. In this respect it resembles Chilko Lake (Desloges and Gilbert, 1998), which is located in a similar setting on the east side of the Coast Range Mountains, and Stave Lake (Gilbert and Desloges, 1992) in the southern Coast Mountains. Therefore, its sedimentary processes and deposits have characteristics of both high-energy glacial lakes such as Lillooet (Gilbert, 1975) and Bower (Gilbert et al., 1997) and lakes (largely intermontane) where sedimentation is much lower and less seasonally dominated (e.g., Pharo and Carmack, 1979). It is significant that the contribution of water and sediment from the Strohn Creek drainage, an area of high-relief mountains with significant glacier cover, completely overwhelms input from the much lower-relief Nass Basin, which has no glaciers, even though it makes up less than half of the area of the drainage basin.

Our study of processes in the lake covers only one season, but the data indicate that inflow is dominated by nival melt and that most of the input of sediment is contributed during a brief period early in the summer. Upon reaching the lake, most of the sediment is deposited within a very short distance from the point of inflow, while distal rates that are significantly less than  $1 \text{ mm yr}^{-1}$  are very low for montane lakes. Low-density turbidity currents, which are most commonly associated with high-energy glacial lakes, occur during the period of peak inflow and persist intermittently throughout the summer. However, they are not sufficiently powerful (because of the relatively low suspended sediment load) to affect any but the proximal region of the lake.

## Acknowledgments

The project was supported with research and equipment grants from the Natural Sciences and Engineering Research Council of Canada. Scott Barnes and Nicole Auty assisted in the field.

## References Cited

- Bale, A. J., 1998: Sediment trap performance in tidal waters: comparison of cylindrical and conical collectors. *Continental Shelf Research*, 18: 1401–1418.
- Ballantyne, C. K., 2002: Paraglacial geomorphology. *Quaternary Science Reviews*, 21: 1935–2017.
- Barnes, S. D. 2003. Investigation of inter-decadal climate variability in northwestern North America, Little Ice Age to present. Ph.D. dissertation. Queen's University, Kingston. 169 pp.
- Beierle, B. D., Lamoureux, S. F., Cockburn, J. M. H., and Spooner, I., 2002: A new method for visualizing sediment particle size distributions. *Journal of Paleolimnology*, 27: 279–283.
- Brune, G. M., 1953: Trap efficiency of reservoirs. *Transactions, American Geophysical Union*, 34: 407–418.
- Butler, R. D. 2001. The physical limnology and sedimentology of montane Meziadin Lake, northern British Columbia, Canada. M.Sc. thesis., Queen's University, Kingston. 169 pp.
- Carmack, E. C., Gray, C. B. J., Pharo, C. H., and Daley, R. J., 1979: Importance of lake-river interaction on seasonal patterns in the general circulation of Kamloops Lake, British Columbia. *Limnology and Oceanography*, 24: 634–644.
- Cayan, D. R., Gardner, J. V., Landwehr, J. M., Namias, J., and Peterson, D. H. (eds.), 1989: Aspects of climate variability in

- the Pacific and the western Americas. *Geophysical Monograph*, 55.
- Church, M., and Ryder, J. M., 1972: Paraglacial sedimentation: a consideration of fluvial processes conditioned by glaciation. *Geological Society of America, Bulletin*, 83: 3059–3072.
- Clague, J. J., and Evans, S. G., 1993: Historic retreat of Grand Pacific and Melbern Glaciers, Saint Elias Mountains, Canada: an analogue for decay of the Cordilleran ice sheet at the end of the Pleistocene? *Journal of Glaciology*, 39: 619–624.
- Clague, J. J., and Mathewes, R. W., 1996: Neoglaciation, glacier-dammed lakes, and vegetation change in northwestern British Columbia, Canada. *Arctic and Alpine Research*, 28: 10–24.
- Corbett, D. M., 1962: Stream-gauging procedure: a manual describing methods and practices of the Geological Survey. *United States Geological Survey, Water Supply Paper* 888.
- Dean, W. E., Jr., 1974: Determination of carbonate and organic matter in calcareous sediments and sedimentary rocks by loss on ignition: comparison with other methods. *Journal of Sedimentary Petrology*, 44: 242–248.
- Desloges, J. R., and Gilbert, R., 1994: The record of extreme hydrological and geomorphological events inferred from glaciolacustrine sediments. In Olive, L. J., Loughran, R. J., and Kesby, J. A. (eds.), *Variability in Stream Erosion and Sediment Transport. International Association of Hydrological Sciences Publication No. 2*, 224: 133–142.
- Desloges, J. R., and Gilbert, R., 1998: Sedimentation in Chilko Lake: a record of the geomorphic environment of the eastern Coast Mountains of British Columbia, Canada. *Geomorphology*, 25: 75–91.
- Droppo, I. G., Leppard, G. G., Flannigan, D. T., and Liss, S. N., 1997: The freshwater floc: a functional relationship of water and organic and inorganic floc constituents affecting suspended sediment properties. *Water Air and Soil Pollution*, 99: 43–54.
- Eaton, B., Church, M., and Ham, D., 2002: Scaling and regionalization of flood flows in British Columbia, Canada. *Hydrological Processes*, 16: 3245–3263.
- Gardner, W. D., 1980: Sediment trap dynamics and calibration: a laboratory evaluation. *Journal of Marine Research*, 38: 17–39.
- Gilbert, R., 1975: Sedimentation in Lillooet Lake, British Columbia. *Canadian Journal of Earth Sciences*, 12: 1697–1711.
- Gilbert, R., 2000: Environmental assessment from the sedimentary record of high latitude fiords. *Geomorphology*, 32: 295–314.
- Gilbert, R., and Desloges, J. R., 1987: Sediments of ice-dammed, self-draining Ape Lake, British Columbia. *Canadian Journal of Earth Sciences*, 24: 1735–1747.
- Gilbert, R., and Desloges, J. R., 1992: The late Quaternary sedimentary record of Stave Lake, southwestern British Columbia. *Canadian Journal of Earth Sciences*, 29: 1997–2006.
- Gilbert, R., and Shaw, J., 1981: Sedimentation in proglacial Sunwapta Lake, Alberta. *Canadian Journal of Earth Sciences*, 18: 81–93.
- Gilbert, R., Desloges, J. R., and Clague, J. J., 1997: The glaciolacustrine sedimentary environment of Bowser Lake in the northern Coast Mountains of British Columbia, Canada. *Journal of Paleolimnology*, 17: 331–346.
- Gilbert, R., Chong, Å., Dunbar, R. B., and Domack, E. W., 2003: Sediment trap records of glacial marine sedimentation at Müller Ice Shelf, Lallemand Fjord, Antarctic Peninsula. *Arctic, Antarctic, and Alpine Research*, 35: 24–33.
- Gustavson, T. C., 1975: Sedimentation and physical limnology in proglacial Malaspina Lake, southeastern Alaska. In Jopling, A. V., and McDonald, B. C. (eds.), *Glaciofluvial and Glaciolacustrine Sedimentation. Society of Economic Paleontologists and Mineralogists, Special Publication No. 23*, 249–263.
- Hamblin, P. F., and Carmack, E. C., 1978: River-induced currents in a fjord lake. *Journal of Geophysical Research*, 83: 885–899.
- Lambert, A., and Giovanoli, F., 1988: Records of riverborne turbidity currents and indications of slope failures in the Rhone delta of Lake Geneva. *Limnology and Oceanography*, 33: 458–468.
- Lambert, A., and Hsü, K. J., 1979: Non-annual cycles of varve-like sedimentation in Walensee, Switzerland. *Sedimentology*, 26: 453–461.
- Lambert, A. M., Kelts, K. R., and Marshall, N. F., 1976: Measurements of density underflows from Walensee, Switzerland. *Sedimentology*, 23: 87–105.
- Lamoureux, S. F., 1994: Embedding unfrozen lake sediments for thin section preparation. *Journal of Paleolimnology*, 10: 141–146.
- Leemann, A., and Niessen, F., 1994: Varve formation and the climatic record in an alpine proglacial lake: calibrating annually-laminated sediments against hydrological and meteorological data. *Holocene*, 4: 1–8.
- Leonard, E. M., 1986: Varve studies at Hector Lake, Alberta, Canada, and the relationship between glacial activity and sedimentation. *Quaternary Research*, 25: 199–214.
- Leonard, E. M., 1997: The relationship between glacial activity and sediment production: evidence from a 4450-year varve record of Neoglaciation at Hector Lake, Alberta, Canada. *Journal of Paleolimnology*, 17: 319–330.
- Lewis, T., Gilbert, R., and Lamoureux, S. F., 2002: Spatial and temporal changes in sedimentary processes in proglacial Bear Lake, Devon Island, Nunavut, Canada. *Arctic, Antarctic, and Alpine Research*, 34: 119–129.
- Mathews, W. H., 1965: Two self-dumping ice-dammed lakes in British Columbia. *Geographical Review*, 55: 46–52.
- Middleton, G. V., 1966: Experiments on density and turbidity currents. II Uniform flow of density currents. *Canadian Journal of Earth Sciences*, 3: 627–637.
- Pharo, C. H., and Carmack, E. C., 1979: Sedimentary processes in a short residence-time intermontaine lake, Kamloops Lake, British Columbia. *Sedimentology*, 26: 523–541.
- Pickrill, R. A., and Irwin, J., 1983: Sedimentation in a deep glacier-fed lake—Lake Tekapo, New Zealand. *Sedimentology*, 30: 63–75.
- Röthlisberger, H., and Lang, H., 1987: Glacial hydrology. In Gurnell, A. M., and Clark, M. J. (eds.), *Glacio-fluvial Sediment Transfer*. Chichester, UK: John Wiley and Sons, 207–284.
- Ryder, J. M., 1989: Climate (Canadian Cordillera). In Fulton, R. J. (ed.), *Quaternary Geology of Canada and Greenland*. Geological Survey of Canada, *Geology of Canada* No. 1: 26–30.
- Ryder, J. M., and Maynard, D., 1991: The Cordilleran Ice Sheet in northern British Columbia. *Géographie physique et Quaternaire*, 45: 355–364.
- Smith, N. D., 1978: Sedimentation processes and patterns in a glacier-fed lake with low sediment input. *Canadian Journal of Earth Sciences*, 15: 741–756.
- Sturm, M., 1979: Origin and composition of clastic varves. In Schluchter, C. (ed.), *Moraines and Varves*, Rotterdam: A. A. Balkema, 281–286.
- Sturm, M., and Matter, A., 1978: Turbidites and varves in Lake Brienz (Switzerland): deposition of clastic detritus by density currents. In Matter, A., and Tucker, M. E. (eds.), *Modern and Ancient Lake Sediments*. Blackwell Scientific Publications, Special Publication of the International Association of Sedimentology, 147–168.
- van Tassel, J., 1981: Silver abyssal plain carbonate turbidite: flow characteristics. *Journal of Geology*, 89: 317–333.
- Ware, D. M., and Thomson, R. E., 2000: Interannual to multidecadal timescale climate variations in the northeast Pacific. *Journal of Climate*, 13: 3209–3220.
- Weirich, F., 1986: The record of density-induced underflows in a glacial lake. *Sedimentology*, 33: 261–277.
- Young, G. J., 1980: Glacier hydrology. In Prowse, T. D., and Ommanney, C. S. L. (eds.), *Northern Hydrology: Canadian Perspective*. Saskatoon: National Hydrology Research Institute, 135–162.

Ms submitted September 2002  
Revised ms submitted May 2003